ELSEVIER

Journal of Nuclear Materials 290–293 (2001) 42–46

journal of nuclear materials

www.elsevier.nl/locate/jnucmat

Solid-state reaction between tungsten and hydrogen-containing carbon film at elevated temperature

K. Ashida [a,*], K. Fujino [b], T. Okabe [b], M. Matsuyama [a], K. Watanabe [a]

[a] *Hydrogen Isotope Research Centre, Toyama University, Gofuku 3190, Toyama 930-8555 Japan*
[b] *Department of Physics, Faculty of Science, Toyama University, Gofuku 3190, Toyama 930-8555, Japan*

Abstract

The solid-state reaction between hydrogen-containing carbon and tungsten was studied by means of infrared, Raman, X-ray photoelectron (XPS) and thermal desorption (TDS) spectroscopies. Infrared and Raman spectroscopies revealed that as-prepared hydrogen-containing films were composed of carbon atoms with sp^2 and sp^3 hybridized orbitals, where hydrogen was bound to carbon as $-CH_3$ and $>CH_2$. Vacuum heating of the carbon films deposited on tungsten caused thermal desorption peaks of hydrogen at about 723 and 1173 K in TDS. The former was accompanied by other desorption of CO, CO_2 and hydrocarbons, whereas the latter was evolved with only a minor amount of CO. It was observed by XPS that the W4f peak began to appear at about 773 K, with an increasing surface composition corresponding to tungsten carbide at 1273 K. These observations indicate that a solid-state reaction between the carbon film and tungsten took place extensively above 973 K to yield an intermetallic compound of W_2C at 1273 K. © 2001 Elsevier Science B.V. All rights reserved.

Keywords: Tungsten; Carbon; Co-deposition; Solid-state reaction; Heat load; Hydrogen

1. Introduction

Low-Z materials such as beryllium, boron and carbon have been widely used in tokamaks to improve plasma confinement parameters by the reduction of radiation losses [1,2]. Their high erosion rates through physical and chemical sputtering, evaporation, etc., however, are giving rise to a serious problem for their use as protective tiles on the inner wall of tokamaks. On the other hand, high-Z materials such as molybdenum and tungsten have attracted great attention to compensate for low-Z materials with their durability against high heat loading and particle fluence [3].

Installation of two or more plasma facing materials is common now in many tokamaks to control plasma–surface interactions, but poses a new problem concerning fuel recycling and inventory, which deeply relate with the physiochemical properties of co-existing layers consisting of low- and high-Z materials. An understanding of the properties of co-existing layers is indispensable for material selection on designing next generation tokamaks.

In the present study, tungsten plates covered with hydrogen-containing carbon films were prepared as model system to simulate changes in physiochemical properties of hydrogen-containing carbon depositing on a tungsten divertor. The properties of the co-existing layers and their changes with heat loading were studied by means of infrared, Raman, X-ray photoelectron (XPS) and thermal desorption (TDS) spectroscopies.

2. Experimental

2.1. Sample preparation

Hydrogen-containing carbon films were prepared on tungsten, silicon and quartz plates by inductive RF discharge [4]. Hereafter, they are denoted as C(H)/W,

---

[*] Corresponding author. Tel.: +81-764 45 6927; fax: +81-764 45 6931.

E-mail address: ashida@hrc.toyama-u.ac.jp (K. Ashida).

PII: S0022-3115(00)00561-4

C(H)/Si and C(H)/SiO_2, respectively, in the present paper. The sample C(H)/W was used for observing solid-state reactions between the hydrogen-containing carbon and tungsten, C(H)/Si for infrared and Raman spectroscopy, and C(H)/SiO_2 for referencing standard. The size of each plate was $10 \times 10 \times 0.5$ mm^3. Methane and ethylene of pure grade were used as working gases for deposition of hydrogen-containing carbon films on these substrates. The gases were purchased from Sumitomo Seika and the purities of both gases were guaranteed as 99.99%. They were used without further purification.

The devices for sample preparation and its procedures were the same as C(H)/Be and C(H)/Mo. They are described elsewhere [4–6].

2.2. Measurements

The change in the total pressure was measured during the discharge and the change in the gas composition was analyzed using a QMS by sampling a part of gas through a variable leak value. The QMS has been calibrated for $H_2, H_2O, CO, CO_2, CH_4$ and C_2H_4 by using high purity gases except H_2O, which was supplied from a wet molecular sieve bed.

The characteristics of deposited carbon films were analyzed by FT–IR and Raman spectroscopies. Namely, the C(H)/Si samples were taken out from the preparation system to air and set into their respective sample holders. The spectra were measured at room temperature with 2 cm^{-1} resolution. Thermal desorption spectra were measured for both C(H)/W and C(H)/SiO_2 samples. They were taken out to air and set into a quartz sample tube of a high vacuum system installed with a pre-calibrated mass spectrometer. The sample was heated linearly with time at a rate of 9 K/min up to 1273 K by use of an electric furnace, where the temperature was measured with a thermocouple attached to the sample tube.

The solid-state reaction between the deposited carbon film and the tungsten substrate was measured by XPS through the change in surface composition with vacuum heating. A C(H)/W sample taken out from the sample preparation system was set into the sample holder for XPS. The system could be evacuated down to 10^{-8} Pa. Then the sample was heated at a given temperature for 10 min and cooled down to room temperature for measurements. The sample could be heated ohmically up to 1273 K, where the temperature was measured with a thermocouple attached to the tungsten substrate.

3. Results and discussion

3.1. Characterization of hydrogen-containing carbon films

To determine the composition of hydrogen-containing films, the changes in total and partial pressures with time were measured by using a pressure gauge and the QMS. Figs. 1 and 2 show typical examples of the changes observed during the discharges in methane and ethylene, respectively. In the case of methane (Fig. 1), the discharge yielded hydrogen and ethylene as the main gaseous products. The hydrogen pressure increased continuously with time, while ethylene pressure reached a maximum and then decreased gradually. At the end of the discharge, the total pressure increased to 48 Pa, while the composition of the gas was 87% H_2, 8% CH_4 and 5% C_2H_4. On the other hand, the discharge of ethylene gave hydrogen and acetylene as the main gaseous products (Fig. 2), but the acetylene formed a peak and disappeared at the end of the discharge, where the gas phase consisted of essentially hydrogen (95%) with a minor amount of ethylene (5%), and the total pressure was 25 Pa. On account of these changes in the gas phase, the compositions of the carbon films prepared were evaluated as [H]/[C] = 1.7 and 1.4 for the methane and ethylene discharges, respectively.

Fig. 3 shows a FT–IR spectrum in the frequency region of the C—H stretch bands [7]. It was observed for

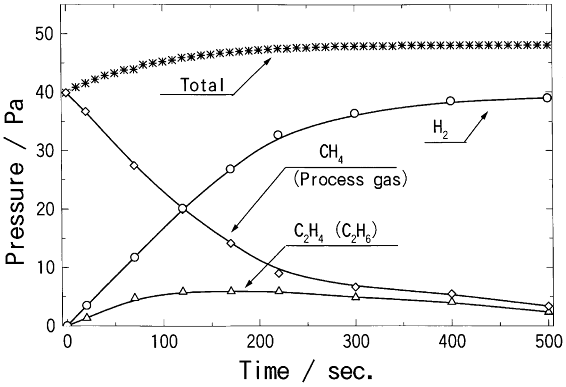

Fig. 1. Pressure changes during discharge of CH_4.

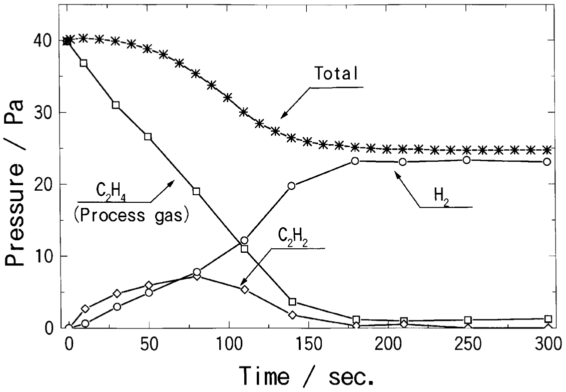

Fig. 2. Pressure changes during discharge of C_2H_4.

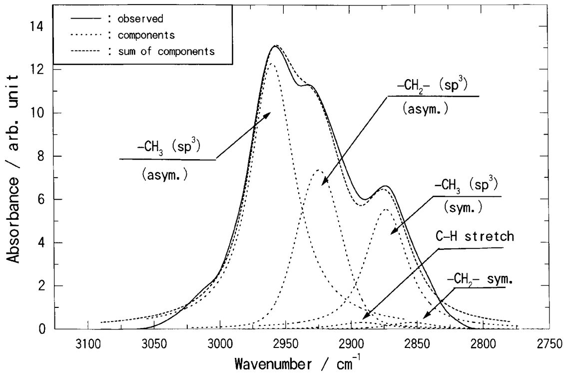

Fig. 3. FT–IR spectrum observed for hydrogen-containing carbon film prepared by a methane discharge.

the film prepared by the methane discharge. Essentially the same spectrum was found for the film prepared by the ethylene discharge. The spectrum could be deconvoluted into three major components, which peaked at 2925, 2875 and 2960 cm^{-1}. They were assigned to symmetric $—CH_3$, asymmetric $>CH_2$ and asymmetric $—CH_3$ stretching vibrations, respectively. Similar band structures were observed for amorphous carbon films [8] and graphite irradiated by keV-energy hydrogen ions [9]. The Raman spectrum of the as-prepared film in a region of 1000–1700 cm^{-1} showed a similar structure to that of so-called amorphous carbon and mainly consisted of two components. One of them peaked at 1300 and the other at 1600 cm^{-1}. The former could be attributed to the C—C single bond and the latter to the C=C double bond. In addition, it should be mentioned that similar Raman spectra have been observed for graphite irradiated with hydrogen ions [10]. On the basis of these observations, it can be concluded that the C—C and C=C bonds make the principle structure of the as-prepared carbon films, which contain hydrogen amounting [H]/[C] = 1.4–1.7 as $—CH_3$ and $>CH_2$.

3.2. Thermal desorption

Fig. 4 shows thermal desorption spectra observed for the C(H)/W film prepared by the methane discharge, where only such species as H_2, CO and H_2O are plotted for simplicity. The relatively high background pressure of H_2O was due to the poor vacuum conditions of the system. The spectra showed two distinct peaks; a low temperature peak centered at about 723 K and a high temperature peak at about 1173 K. In the low temperature region, other species attributable to hydrocarbons such as CH_x, C_2H_x, and C_3H_x formed peaks of similar intensities as CO. On the other hand, the H_2 peak asserted its preeminence over CO in the high temperature region, where no hydrocarbon peaks appeared at all. It should be mentioned that desorption peak at the low temperature region was also observed for the C(H)/SiO_2 samples, whereas no high temperature H_2 peak appeared. Similar phenomena have been also observed for C(H)/Mo [6] and C(H)/Be [4], although the peak temperatures differ from each other. Small peaks of H_2 and CO observed at about 910 K were ascribed to the tungsten substrate, because they also appeared from a tungsten plate but not from a quartz glass plate and the sample tube itself. These peaks were presumably due to reactions of surface contaminants of the tungsten plate (O and C) and water vapor in the system.

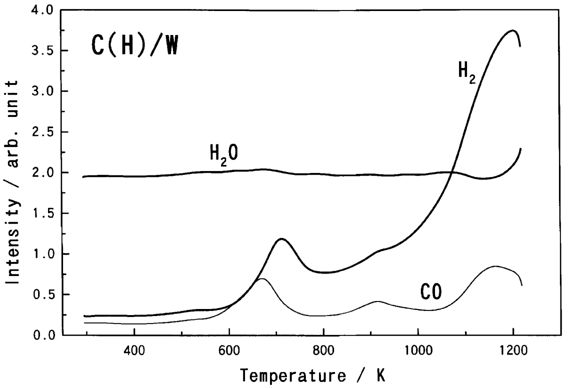

Fig. 4. Thermal desortion spectra of predominant species for a C(H)/W film.

3.3. Change in surface composition

The surface composition of the carbon films and the chemical state of surface elements were analyzed by XPS to observe their changes with heat loading. The sample was heated in vacuum at a given temperature for 10 min, and cooled down to room temperature for measurement. Similar procedures were repeated step by step up to 1273 K. Fig. 5 shows the change in the surface compo-

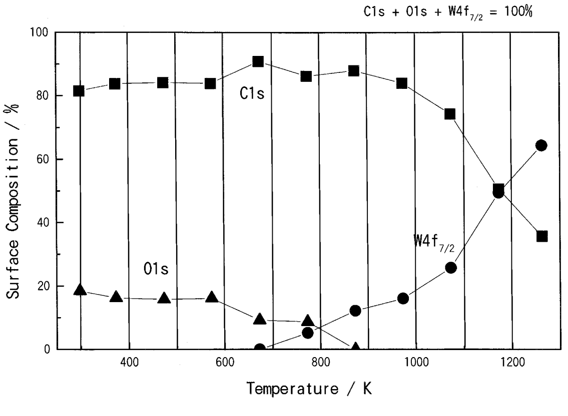

Fig. 5. Change in surface composition with vacuum heating of C(H)/W prepared by a methane discharge.

sition of the sample prepared by the methane discharge. It is seen that the surface composition was almost constant below 600 K. Above 600 K, the oxygen concentration started to decrease and disappeared at 873 K. The carbon concentration began to decrease at 973 K and reached 36% at 1273 K. On the contrary, tungsten appeared only after the heating at 773 K and then increased to 64% at 1273 K. Similar phenomena have been observed for C(H)/Be [5] and C(H)/Mo [6].

On the basis of TDS and XPS observations, it is concluded that a solid-state reaction between the film and the substrate plays an essential role for the hydrogen evolution and the formation of W_2C in the high temperature region. The formation of W_2C was confirmed by not only the surface composition but also by the chemical shifts of $W4f_{7/2}$ and C1s peaks in XPS as well as X-ray diffraction.

3.4. Hydrogen evolution mechanism

As to the hydrogen evolution in the low temperature region, no appreciable desorption should be expected because of the high bond energy of C—H [11]. In fact, hydrogen ion-implanted graphite shows hydrogen desorption peaks above 923 K [12]. The hydrogen evolution in the low temperature region shown in Fig. 4 can be ascribed to reactions between the film and water adsorbed as $H_2O(a)$ and/or OH(a), because the O1s peak from OH(a) disappeared from XPS spectra around 573 K, although the O1s peak attributable to CO(a) still remained on the surface till 773 K. Therefore, the hydrogen evolution in the low temperature region should be described as

$$[\text{—CH}_n\text{—}]_m + x\text{H}_2\text{O(a)} \rightarrow x\text{C(O)} + (x + m'n'/2)\text{H}_2 \quad (1)$$

$$[\text{—CH}_n\text{—}]_m + x\text{OH(a)} \rightarrow x\text{C(O)} + ((x + m'n')/2)\text{H}_2 \quad (2)$$

$$(n = 0 \sim 3, n > n', m > m')$$

$$\text{C(O)} \rightarrow \text{CO(gas)} \quad (3)$$

where $[\text{—CH}_n\text{—}]_m$ represents the hydrogen-containing carbon, $H_2O(a)$ and OH(a) an adsorbed water and a hydroxyl molecules, respectively, and C(O) a carbon site occupied by adsorbed oxygen. The adsorbed $H_2O(a)$ and OH(a) molecules appear to arise partly from the air exposure of the sample during the transfer from the preparation apparatus to the XPS system and partly from the presence of residual water vapor in the TDS system.

On the contrary, the hydrogen release in the high temperature region is due to the solid-state reaction of the carbon film with the substrate to form W_2C, which was identified by X-ray diffraction analysis. On the basis of these observations, it can be concluded that the solid-state reaction between them is described as

$$[\text{—CH}_n\text{—}]_m + y\text{W} \rightarrow (y/2)\text{W}_2\text{C} + (m'n')\text{H(a)} \quad (4)$$

$$(n = 0 \sim 3, n > n', m > m')$$

It is also plausible that a part of tungsten appearing on the surface reacts with water vapor present in the system as residual gas to form tungsten oxide. It can then react with the carbon film as

$$\text{W} - \text{oxide} + [\text{—CH}_n\text{—}]_m \rightarrow \text{W} + \text{CO(gas)} + (m'n')\text{H(a)} \quad (5)$$

Subsequently, the adsorbed hydrogen desorbs from the surface, but a small part may dissolve in the tungsten substrate. Namely, the hydrogen release reaction is described as

$$(m'n')\text{H(a)} \rightarrow \alpha\text{H}_2 + \beta\text{H(s)}, \quad (2\alpha + \beta = m'n') \quad (6)$$

These reaction schemes are essentially the same as those proposed for the solid-state reaction between hydrogen-containing carbon and molybdenum [6].

3.5. Effect of substrate material

As mentioned above, C(H)/Be, C(H)/Be, C(H)/Mo and C(H)/W give the respective metallic carbides as Be_2C [4,5], Mo_2C [6] and W_2C by vacuum heating. The ease of carbide formation, however, differs considerably from each other. For example, Table 1 shows the difference in the hydrogen desorption peaks in the low and high temperature regions. It can be seen that the peak temperature in the high temperature region increases with increasing atomic number of the substrate material, whereas the one in the low temperature region is kept almost constant around 723 K for each substrate.

Table 2 shows another example of the substrate dependence of the solid-state reaction observed by XPS, where one of the characteristic temperature was defined as the temperature at which the ratio, [C]/[M], became equal, and the other was the temperature at which the ratio attained to [C]/[M] = 1/2, corresponding to the completion of carbide formation as M_2C, where M denotes Be, Mo or W. Hereafter, they are denoted as the halfway and the completion temperatures, respectively. Both of them increased with an increase in the atomic number of substrate materials.

Table 1
Comparison of H_2 desorption peak temperatures in the low and high temperature regions

	Low temp. (K)	High temp. (K)
C(H)/W	723	1173
C(H)/Mo	703	1050
C(H)/Be	723	873
C(H)/SiO_2	713	None

Table 2
Comparison of characteristic temperatures defined by [H]/[M] ratios determined by XPS

	C(H)/W	C(H)/Mo	C(H)/Be
Halfway temp. (K)	1173	1073	823
Compl. temp. (K)	1273	1173	873

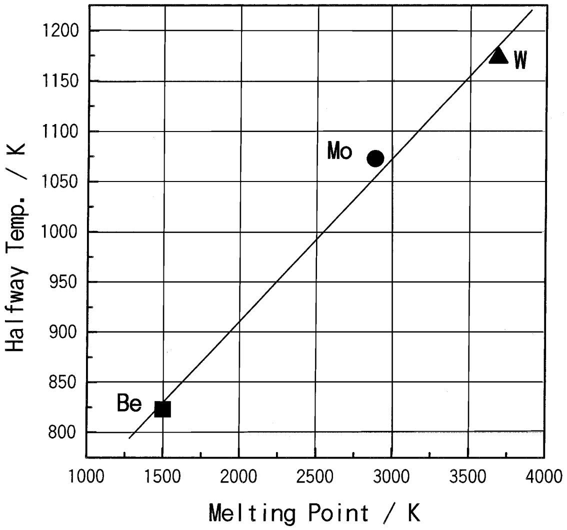

Fig. 6. Plots of the halfway temperature againt the melting points of substrate materials.

The halfway temperatures are plotted in Fig. 6 against the melting points of substrate materials. It resulted in a good straight line. A similar relation was found for the completion temperature. Namely the solid-state reaction and the hydrogen evolution become progressively faster on the substrate having a lower melting point. In addition, it is worthwhile to mention that the solid-state reaction appears not to be due to a diffusion limited process, because the diffusion constants of carbon in molybdenum and tungsten are almost equivalent [13] and no appreciable difference between them should be expected for the characteristic temperatures and the hydrogen desorption peak temperature. In fact, the solid-state reaction for C(H)/Be has been explained well [5] by a random nucleation and subsequent growth model [14,15].

4. Conclusions

The following conclusions were obtained for the physicochemical properties of hydrogen containing carbon deposited on tungsten and the solid-state reaction between them by means of FT–IR, Raman, thermal desorption and X-ray photoelectron spectroscopies along with X-ray diffraction analysis.

1. The hydrogen-containing carbon films prepared by plasma CVD in methane and ethylene consisted of C—C and C=C bondings comprising sp^2 and sp^3 hybridized orbitals. Hydrogen was principally bound to carbon as $>CH_2$ and $-CH_3$.
2. The vacuum heating of the carbon films formed the desorption peaks of hydrogen about 723 and 1173 K in TDS spectra. The former could be ascribed to reactions of hydrogen containing carbon with adsorbed hydroxyl and/or water molecules. The latter was attributed to a solid-state reaction between hydrogen-containing carbon and tungsten, which yielded H_2 and W_2C as reaction products.
3. A linear relation was found between the solid-state reactivity of hydrogen-containing carbon and the melting point of substrate material among C(H)/M, where M indicates Be, Mo or W. This relation strongly suggests that the solid-state reaction is not due to a diffusion limited process, but attributable to a random nucleation and subsequent growth mechanism.

References

[1] R. Behrisch, A.P. Martinelli, S. Grigull, R. Grotzschel, D. Hildebrandt, W. Schneider, J. Nucl. Mater 220–222 (1995) 590.
[2] A. Sagara et al., J. Nucl. Mater 241–243 (1997) 972.
[3] V. Philipps, R. Nue, J. Nucl. Mater 241–243 (1997) 227.
[4] K. Ashida, K. Watanabe, T. Okabe, J. Nucl. Mater 241–243 (1997) 1060.
[5] K. Ashida, K. Watanabe, Fus. Eng. Des. 37 (1997) 307.
[6] K. Ashida, K. Watanabe, I. Kitamura, S. Ikeno, J. Nucl. Mater 266–269 (1999) 434.
[7] B. Dischler, E-MRS Meeting, June 1989, vol. XVII, p. 189.
[8] S. Chiu, S. Turgeon, B. Terreaul, A. Sarkissian, Thin Solid Films 359 (2000) 275.
[9] Y. Gotoh, S. Kajiura, J. Nucl. Mater. 266–269 (1999) 1051.
[10] K. Ashida, K. Kanamori, M. Matsuyama, K. Watanabe, J. Nucl. Mater 137 (1986) 288.
[11] R.C. Weast, M.J. Astle (Eds.), CRC Handbook of Chemistry and Physics, 62nd Ed., Boca Raton, FL, 1981.
[12] K. Ashida, K. Ichimura, M. Matsuyama, K. Watanabe, J. Nucl. Mater 128–129 (1984) 972.
[13] Japan Institute Metals, Metal Databook, 2nd Ed., Muruzen, Tokyo, Japan, 1984.
[14] J.H. Sharp, G.W. Brindely, B.N. Narahari Achar, J. Am. Ceram. Soc. 49 (1966) 379.
[15] S.F. Hulbert, J. Br. Ceram. Soc. 6 (1969) 11.